Available online at www.sciencedirect.com

ScienceDirect

International Journal of Solids and Structures 45 (2008) 821–839

INTERNATIONAL JOURNAL OF SOLIDS AND STRUCTURES

www.elsevier.com/locate/ijsolstr

Effect of the rate dependence of nonlinear kinematic hardening rule on relaxation behavior

Kwangsoo Ho *

Department of Mechanical Engineering, Keimyung University, 1000 Sindang-Dong, Dalseo-Gu, Daegu, 704-701, South Korea

Received 7 May 2007; received in revised form 28 August 2007
Available online 14 September 2007

Abstract

Relaxation experiments for metallic materials and solid polymers have exhibited nonlinear dependence of stress relaxation on prior loading rate; the relaxed stress associated with the fastest prior strain rate has the smallest magnitude at the end of the same relaxation periods. Modeling capability for the basic feature of relaxation behavior is qualitatively investigated in the context of unified state variable theory. Unified constitutive models are categorized into three general classes according to the rate dependence of kinematic hardening rule, which defines the evolution of the back (equilibrium) stress and is the major difference among constitutive models. The first class of models adopts the nonlinear kinematic hardening rule proposed by Armstrong and Frederick. In this class, the back stress appears to be rate-independent under loading and subsequent relaxation conditions. In the second class of models, a stress rate term is incorporated into the Armstrong–Frederick rule and the back stress then becomes rate-dependent during relaxation condition even though it remains rate-independent under loading condition. The final class proposed here includes a new nonlinear kinematic hardening rule that causes the back stress to be rate-dependent all the time. It is shown that the apparent rate dependence of the back stress during relaxation enables constitutive models to predict the influence of prior loading rate on relaxation behavior.

Keywords: Viscoplasticity; Nonlinear kinematic hardening rule; Relaxation

1. Introduction

Relaxation test consists of loading with a constant strain rate up to a certain strain that is kept constant during relaxation. Repeated relaxation tests on A533B steel at room temperature under strain control, using piecewise constant strain rates between $10^{-6}\,s^{-1}$ and $10^{-3}\,s^{-1}$ and relaxation periods of 900s duration, exhibited that the stress drop increased with prior strain rate (Krempl and Kallianpur, 1984). Monotonic tensile tests with intermittent relaxation periods of 1048s duration were performed on modified 9Cr–1Mo steel at 538 °C for a fast ($6.25\times10^{-4}\ s^{-1}$) and a slow ($6.9\times10^{-6}\ s^{-1}$) strain rate (Majors and Krempl, 1994).

* Tel.: +82 53 580 5546; fax: +82 53 580 6285.
E-mail address: hok@kmu.ac.kr

0020-7683/$ - see front matter
doi:10.1016/j.ijsolstr.2007.09.003

The experiment revealed that the test associated with the fastest prior strain rate had the smallest stress magnitude at the end of the relaxation period.

Experimental observations for the influence of prior strain rate on relaxation behavior were found on solid polymers as well as metallic materials (Bordonaro and Krempl, 1992; Khan and Farrokh, 2006; Yaguchi and Takahashi, 1999, 2000; Yaguchi et al., 2002). From the experimental evidence, it is concluded that the relaxed stress associated with a faster prior strain rate has a smaller magnitude at the end of relaxation test of equal duration. Thus, when materials experience positive strain rate sensitivity of the flow stress, meaning the flow stress nonlinearly increases with strain rate, the stress drop during relaxation period increases with an increase of prior strain rate, see Krempl and Nakamura (1998) and Krempl (2001) for a summary.

A great deal of research has been performed to develop a unified phenomenological model, considering only one inelastic strain, for various inelastic deformation responses under complex loading conditions. Based on the framework of continuum mechanics, the majority of constitutive models introduce a few of internal state variables that are normally considered to be repositories of the changing microstructure. One of the main differences among the constitutive models is the kinematic hardening rule that describes the evolution of the back (equilibrium) stress in inelastic deformation processes.

Nonlinear kinematic hardening rule was first proposed by Armstrong and Frederick (1966) who introduced a recall term, associated with an evanescent strain memory effect (dynamic recovery), in classical linear kinematic hardening rule (Prager, 1956) so as to represent the initial nonlinearity of hysteresis curve. To improve modeling capabilities for hysteresis curve, Chaboche and Rousselier (1983) decomposed the back stress into several independent variables, each of them being of the nonlinear kinematic hardening rule. As a superposition of the several hardening rules, the decomposed nonlinear kinematic hardening rule seems to be more effective in controlling the speed of saturation of kinematic hardening (Chaboche, 1986; Chaboche and Nouailhas, 1989; Lemaitre and Chaboche, 1994). Based on a superposition of several nonlinear kinematic hardening rules, Ohno and Wang (1993) also introduced a critical state of dynamic recovery in order to improve a description of ratchetting effect. The dynamic recovery of the nonlinear kinematic hardening rule takes place only in a critical state, which is contrasted to the models before mentioned (Ohno and Abdel-Karim, 2000). On the other hand, Krempl et al. (1986) introduced a stress rate term into the nonlinear kinematic hardening rule. The inclusion of the new term was purposed to improve the modeling capability for the initial quasi-elastic region of stress–strain curve since their constitutive equations did not employ a yield surface (Krempl, 1996; Colak and Krempl, 2003). Nonlinear kinematic hardening rule with a stress rate term has been adopted by other researchers to describe inelastic deformation behavior satisfactorily (Phillips et al., 1974; Ramaswamy et al., 1990; Basuroychowdhury and Voyiadjis, 1998). Ho (2001, 2004, 2006) proposed a rate-dependent nonlinear kinematic hardening rule in order to consistently depict positive, zero and negative rate sensitivities of the flow stress. The negative rate sensitivity, in which the flow stress decreases with an increase of loading rate, is concerned with dynamic strain aging depending on a certain range of strain, strain rate and temperature.

In order to investigate the influence of the kinematic hardening rule on the relaxation behavior, the unified phenomenological constitutive models are categorized into three classes. The classification is accomplished by examining whether or not the back (equilibrium) stress apparently exhibits rate dependence under loading and relaxation conditions. Each class is qualitatively evaluated through numerical experiments for relaxation behavior.

2. Modeling capability for relaxation

We assume small strain, isotropy, and volume preserving inelastic deformation. The stress and strain tensors are $\boldsymbol{\sigma}$ and $\boldsymbol{\varepsilon}$, respectively, and $\mathbf{s}$ and $\mathbf{e}$ are their respective deviators. The total strain rate is assumed to be the sum of the elastic and inelastic strain rates. The flow law is thus given by

$$\dot{\mathbf{e}} = \dot{\mathbf{e}}^{\mathrm{el}} + \dot{\mathbf{e}}^{\mathrm{in}} = \frac{1+\nu}{E}\dot{\mathbf{s}} + \frac{3}{2}\dot{\phi}\frac{(\mathbf{s}-\mathbf{g})}{J(\boldsymbol{\sigma}-\mathbf{G})} \tag{1}$$

where E and v are the elastic modulus and Poisson's ratio, respectively. $\mathbf{g}$ is the deviatoric back stress that is a tensor valued state variable of constitutive equations. A superposed dot designates material time derivative. The effective inelastic strain rate $\dot{\phi}$ and the overstress invariant $J(\boldsymbol{\sigma}-\mathbf{G})$ are defined as follows:

$$\dot{\phi}=\sqrt{\frac{2}{3}\mathrm{tr}(\dot{\mathbf{e}}^{\mathrm{in}}\dot{\mathbf{e}}^{\mathrm{in}})} \tag{2}$$

$$J(\boldsymbol{\sigma}-\mathbf{G})=\sqrt{\frac{3}{2}\mathrm{tr}[(\mathbf{s}-\mathbf{g})(\mathbf{s}-\mathbf{g})]} \tag{3}$$

where the trace is denoted by tr; $\mathrm{tr}(\mathbf{ab})=a_{ij}\,b_{ij}$. The deviatoric formulation is augmented by the volumetric elastic deformation:

$$\mathrm{tr}(\dot{\boldsymbol{\varepsilon}})=\frac{1-2v}{E}\mathrm{tr}(\dot{\boldsymbol{\sigma}}) \tag{4}$$

The evolution of the back stress is described by kinematic hardening rule. In order to evaluate the influence of the back stress on modeling of relaxation features, kinematic hardening rules are distinguished from their rate sensitivity under loading and subsequent relaxation conditions; kinematic hardening rules are divided into rate-independent and rate-dependent one during loading, and the former class is again divided into two branches which depend on whether the back stress is considered rate-independent or rate-dependent with respect to prior strain rate during relaxation behavior.

2.1. Rate-independent NLK model

Nonlinear kinematic hardening rule proposed by Armstrong and Frederick consists of the strain hardening and dynamic recovery terms. The majority of unified phenomenological constitutive models have chosen and then have modified this hardening rule as the evolution law for the back stress in order to perform more accurate prediction of inelastic deformation behavior. Rate independence of the back stress seems to be one of the main characteristics of the constitutive models. Among these are the kinematic hardening rules of Chaboche and Ohno–Wang models.

The kinematic hardening rule proposed by Armstrong and Frederick is given in the form (Lemaitre and Chaboche, 1994):

$$\dot{\mathbf{g}}=\frac{2}{3}C\dot{\mathbf{e}}^{\mathrm{in}}-\gamma\mathbf{g}\dot{\phi} \tag{5}$$

where C and γ are material constants. The effective inelastic strain rate $\dot{\phi}$ is defined by

$$\dot{\phi}=\sqrt{\frac{2}{3}\mathrm{tr}(\dot{\mathbf{e}}^{\mathrm{in}}\dot{\mathbf{e}}^{\mathrm{in}})}=\left\langle\frac{[J(\boldsymbol{\sigma}-\mathbf{G})-A]}{K}\right\rangle^{m} \tag{6}$$

where A, K and m are material constants. $<>$ is Macauley's bracket and means that $\langle x\rangle=(x+|x|)/2$.

For monotonic tensile loading, the constitutive equations are then reduced to

$$\dot{\varepsilon}=\dot{\varepsilon}^{\mathrm{el}}+\dot{\varepsilon}^{\mathrm{in}}=\frac{\dot{\sigma}}{E}+\dot{\phi} \tag{7}$$

$$\dot{G}=C\dot{\varepsilon}^{\mathrm{in}}-\gamma G\dot{\phi} \tag{8}$$

where the effective inelastic strain rate reduces to $\dot{\phi}=\dot{\varepsilon}^{\mathrm{in}}=\langle(\sigma-G-A)/K\rangle^{m}$ using $J(\boldsymbol{\sigma}-\mathbf{G})=|\sigma-G|$ and $\sigma-G\geqslant 0$. The evolution equation of the back stress can be analytically integrated to give:

$$G=\frac{C}{\gamma}(1-\mathrm{e}^{-\gamma\varepsilon^{\mathrm{in}}}) \tag{9}$$

The above relation shows that the back stress stabilizes to a value of $\{G\}=C/\gamma$ after undergoing some amount of inelastic strain; the symbol $\{\}$ denotes the long-time asymptotic value of a quantity. This asymptotic solution is thought to apply when inelastic flow is fully established. Thus the back stress is considered to be rate-independent in fully established inelastic flow region.

Loading with a constant strain rate is performed up to a certain strain that is then kept constant for relaxation test. During the relaxation period, the strain rate is set to zero and Eq. (8) then reduces to

$$\dot{G} = \frac{E_t}{E}|\dot{\sigma}| \tag{10}$$

where the inelastic modulus is defined by $E_t = C - \gamma G$. To arrive at Eq. (10), we have made use of $\dot{\varepsilon}^{\text{in}} = -\dot{\varepsilon}^{\text{el}} = -\dot{\sigma}/E$. The above relation describes that the back stress increases or stays constant when $E_t = 0$. It is assumed that the relaxation test starts at a certain strain in the region of fully developed inelastic flow where the inelastic modulus E_t is much smaller than the elastic modulus E. Using the general condition of $E_t \ll E$, the change of the back stress becomes a fraction of that of the stress. The back stress can be then assumed to keep constant during relaxation period because its variation is a negligibly small amount.

The stress rate $\dot{\sigma} = -E\langle(\sigma - G - A)/K\rangle^m$ is obtained from Eq. (7), so that the stress drop during relaxation terminates when the condition $\sigma = G + A$ is reached. Since the back stress G and the material constant A are all rate-independent the relaxed stresses of the same strain level with different prior strain rates end up one point finally, which means no effect of prior strain rate on the relaxed stress magnitude at the end of equal relaxation periods.

Fig. 1 is the result for loading with constant strain rates up to $\varepsilon = 0.03$ that is then kept constant during relaxation tests. The material constants used for numerical experiment are:

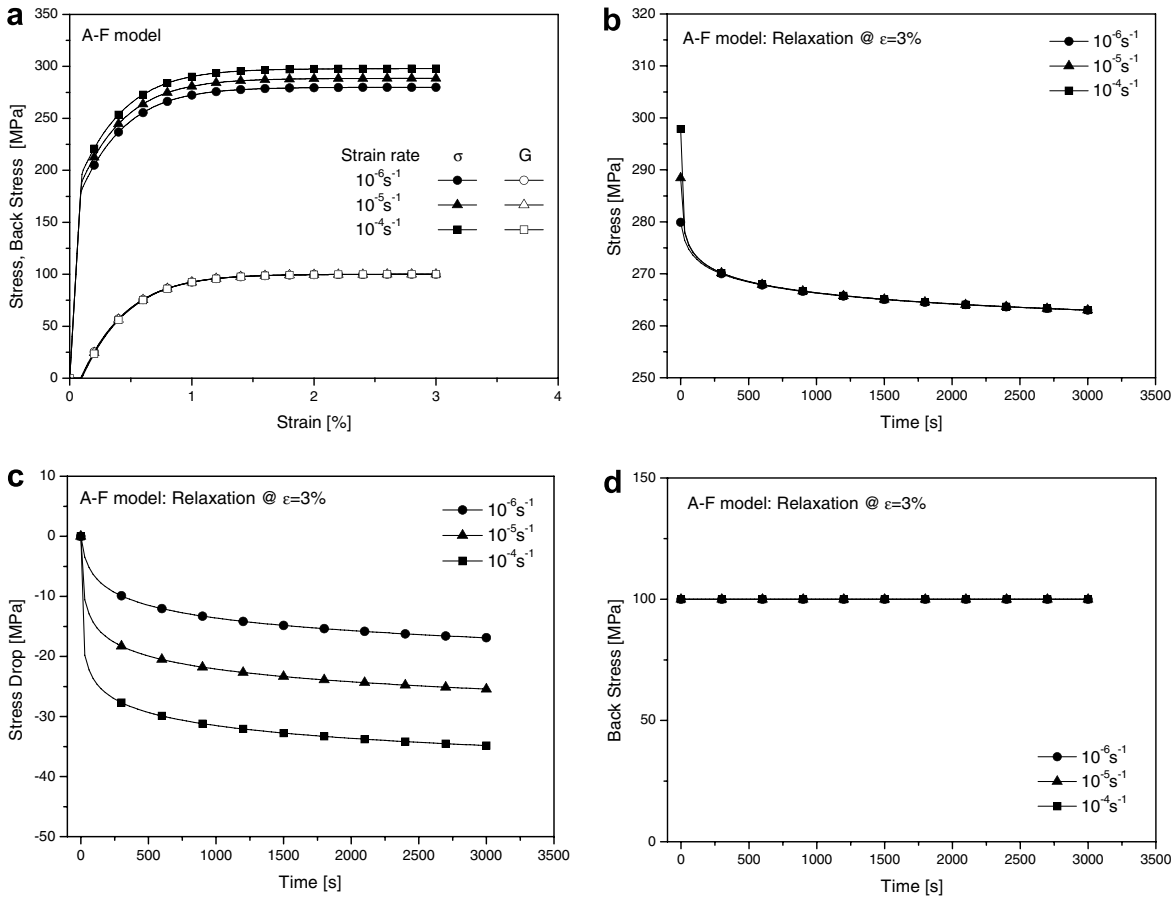

Fig. 1. Numerical experiments by Armstrong–Frederick model. (a) Stress and rate-independent back stress; (b) no influence of prior strain rate on relaxed stress; (c) stress drop versus time; (d) rate-independent back stress during relaxation.

$$E = 200\ \text{GPa}, \quad K = 151\ \text{MPa}, \quad A = 95\ \text{MPa}, \quad m = 24$$
$$C = 30\ \text{GPa}, \quad \gamma = 300$$

Fig. 1a depicts the stress and the back stress plotted for each strain rate. The flow stress exhibits positive rate sensitivity. But the back stress appears to be rate-independent as expected from Eq. (9). Beyond strains of approximately 1% the back stress starts to stabilize and the inelastic modulus E_t consequently becomes zero. The relaxation curves in Fig. 1b exhibit that all relaxed stresses for different prior strain rates are equal at the end of relaxation periods. On the other hand, it is seen from Fig. 1c that the magnitude of stress drop increases with prior strain rate since the flow stress experiences positive rate sensitivity at the start of relaxation test. The back stress during relaxation is plotted in Fig. 1d. As explained in Eq. (10) with $E_t = 0$, the magnitude of the back stress does not change all through relaxation period, and consequently, the back stress remains rate-independent all the time. There is no influence of prior strain rate on stress level at the end of relaxation period.

The Chaboche hardening rule is a superposition of several Armstrong and Frederick kinematic hardening rules in the form (Chaboche, 1986; Chaboche and Nouailhas, 1989):

$$\dot{\mathbf{g}}_i = \frac{2}{3} C_i \dot{\mathbf{e}}^{\text{in}} - \gamma_i \mathbf{g}_i \dot{\phi} \tag{11}$$

where $\dot{\phi} = \langle [J(\boldsymbol{\sigma} - \mathbf{G}) - A]/K \rangle^m$ is the effective inelastic strain rate; C_i and γ_i are material constants. The back stress $\mathbf{G}$ consists of N parts.

In uniaxial tensile loading, the back stress evolves in a rate-independent form as follows:

$$G = \sum_{i=1}^{N} G_i = \sum_{i=1}^{N} \frac{C_i}{\gamma_i} (1 - \mathrm{e}^{-\gamma_i \varepsilon^{\text{in}}}) \tag{12}$$

As $\varepsilon^{in} \to \infty$, the above relation becomes $\{G_i\} = C_i/\gamma_i$. Using the relaxation condition $\dot{\varepsilon} = 0$, Eq. (11) can be rewritten as

$$\dot{G} = \frac{E_t}{E} |\dot{\sigma}|; \quad E_t = \sum_{i=1}^{N} (C_i - \gamma_i G_i) \tag{13}$$

The change of the back stress during relaxation can be negligible due to $E_t \ll E$.

Fig. 2 shows numerical experiment by the Chaboche model ($N = 2$) using the following material constants:

$$E = 200\ \text{GPa}, \quad A = 118\ \text{MPa}, \quad K = 120\ \text{MPa}, \quad m = 11$$
$$C_{1,2} = 120, 3\ \text{GPa}, \quad \gamma_{1,2} = 2000, 0.5$$

It is observed in Fig. 2a that when the stress–strain curves become equidistant beyond strains of around 0.5%, the inelastic flow may be regarded as fully established; while the first back stress (G_1) evolves with a very large modulus and stabilizes quickly, the second back stress (G_2) depicts the subsequent linear part of the stress–strain curve with a relatively very small value of γ_2. The stresses during relaxation test are plotted against time in Fig. 2b. The relaxed stresses at the end of relaxation have one endpoint regardless of the prior strain rate. Since the ratio of the inelastic modulus E_t to the elastic modulus E is about 1.6% at $\varepsilon = 3\%$, the back stress hardly changes during relaxation period. The result is shown in Fig. 2c.

As a decomposed nonlinear kinematic hardening rule, the Ohno–Wang hardening rule introduces a critical state of dynamic recovery (Ohno and Wang, 1993; Ohno and Abdel-Karim, 2000). The evolution of each back stress can be expressed as

$$\dot{\mathbf{g}}_i = \zeta_i \left[\frac{2}{3} \rho_i \dot{\mathbf{e}}^{\text{in}} - \mu_i \mathbf{g}_i \dot{\phi} - L(f_i) \langle \dot{\lambda}_i \rangle \mathbf{g}_i \right] \tag{14}$$

where ζ_i, ρ_i and $0 \leqslant \mu_i \leqslant 1$ are material constants, L stands for the Heaviside's step function, and $\dot{\phi} = B \sin h \langle [J(\boldsymbol{\sigma} - \mathbf{G}) - A]/K \rangle$ is the effective inelastic strain rate. The critical surface is defined by $f_i = (3/2)\mathrm{tr}(\mathbf{g}_i\, \mathbf{g}_i) - (\rho_i)^2$. The third term on the right hand side in Eq. (14) takes place on the critical surface $f_i = 0$. Using the consistency condition $\dot{\lambda}_i$ is given in the form:

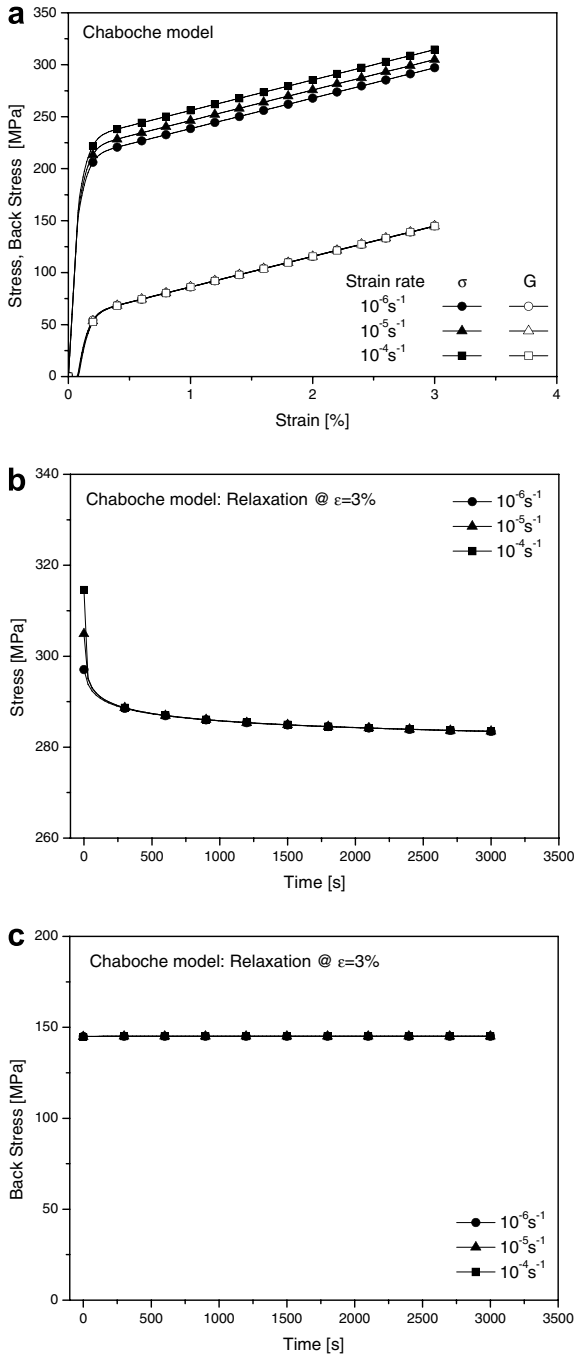

Fig. 2. Numerical experiments by Chaboche model. The back stress is rate-independent during both loading and relaxation. The relaxed stresses end up at one endpoint as shown in (b).

$$\dot{\lambda}_i = \mathrm{tr}[\dot{\mathbf{e}}^{\mathrm{in}}(\mathbf{g}_i/\rho_i)] - \mu_i\dot{\phi} \tag{15}$$

To elucidate essential features of the model, let us consider monotonic tensile loading. Under the loading condition, the back stress becomes

$$G = \sum_{i=1}^{N} G_i = \sum_{i=1}^{N} \rho_i \left[1 - \left\langle 1 - \frac{1}{\mu_i} (1 - \mathrm{e}^{-\mu_i \zeta_i \dot{e}^{\mathrm{in}}}) \right\rangle \right] \tag{16}$$

The long-time asymptotic value of the back stress is determined to be $\{G_i\} = \rho_i$. The back stress growth rate under relaxation condition can be expressed in the form:

$$\dot{G} = \frac{E_t}{E} |\dot{\sigma}|; \quad E_t = \sum_{i=1}^{N} \zeta_i \left[\rho_i - \mu_i G_i - L(f_i) \left\langle \frac{G_i}{\rho_i} - \mu_i \right\rangle G_i \right] \tag{17}$$

Using $E_t \ll E$, it may be agreed that the back stress hardly change during relaxation period.

The results in Fig. 3 for $N = 10$ are obtained with the following material constants:

$$E = 200 \text{ GPa}, \quad A = 75 \text{ MPa}, \quad K = 6.2 \text{ MPa}, \quad \mu_i = 0.01, \quad B = 2.48 \times 10^{-10}\ s^{-1}$$
$$\zeta_{1-10} = 10000, 5000, 2500, 1000, 400, 184, 100, 50, 33.3, 25$$
$$\rho_{1-10} = 10, 14, 17.3, 22, 20.6, 14.7, 6.4, 10, 9, 80 \text{ MPa}$$

The rate-independent growth of the back stress and the same endpoint of the relaxed stresses are shown in Fig. 3a and b, respectively. As expected in Eq. (17), the back stress is regarded as to be independent of prior strain rate since the ratio E_t/E is about 1.2% at the strain that the relaxation takes place.

In the rate-independent NLK models, the back stress appears to be rate-independent under relaxation condition as well as loading condition. These models can depict that the magnitude of stress drop during relaxation increases with an increase in prior strain rate. However, they do not predict that the relaxed stress related to a faster prior strain rate has a smaller magnitude at the end of relaxation periods due to the rate-independent property of the back stress.

2.2. Rate-independent NLK model with a stress rate term

Nonlinear kinematic hardening rule includes a stress rate term as well as the two competing strain hardening and dynamic recovery terms. Among this class of constitutive models, the viscoplasticity theory based on overstress (VBO) model developed by Krempl and his coworkers is considered to illustrate the properties of relaxation behavior qualitatively. The evolution of the back stress is given in the form (Krempl, 1996, 2001; Colak and Krempl, 2003):

$$\dot{\mathbf{g}} = \frac{\psi}{E} \dot{\mathbf{s}} + \psi \left[\frac{2}{3} \dot{\mathbf{e}}^{\mathrm{in}} - \frac{(\mathbf{g} - \mathbf{h})}{A} \dot{\phi} \right] + \left(1 - \frac{\psi}{E} \right) \dot{\mathbf{h}} \tag{18}$$

where A is a material constant and the effective inelastic strain rate is defined by $\dot{\phi} = B[J(\boldsymbol{\sigma} - \mathbf{G})/K]^m$. The shape function ψ is bounded by $E_t \ll \psi < E$. It controls the transition from initial quasi-elastic behavior to fully developed inelastic flow. For the proper modeling of the initial quasi-elastic region without a concept of yield surface, the shape function is usually chosen close to the elastic modulus. The kinematic stress is introduced to describe work hardening in monotonic loading and its evolution is given in the Prager hardening form by

$$\dot{\mathbf{h}} = \frac{2}{3} E_t \dot{\mathbf{e}}^{\mathrm{in}} \tag{19}$$

where E_t is a material constant and is the inelastic modulus at the maximum inelastic strain of interest. The kinematic stress defined by the linear hardening rule evolves in a rate-independent fashion.

In tensile loading case, the asymptotic relation $\{\dot{\sigma}\} = \{\dot{G}\} = \{\dot{H}\}$ holds for large times. We see that the evolution of the kinematic stress sets the slope of the stress and back stress curves against strain in the region of asymptotic state. An asymptotic limit for the difference of the back stress and the kinematic stress can be obtained from Eq. (18):

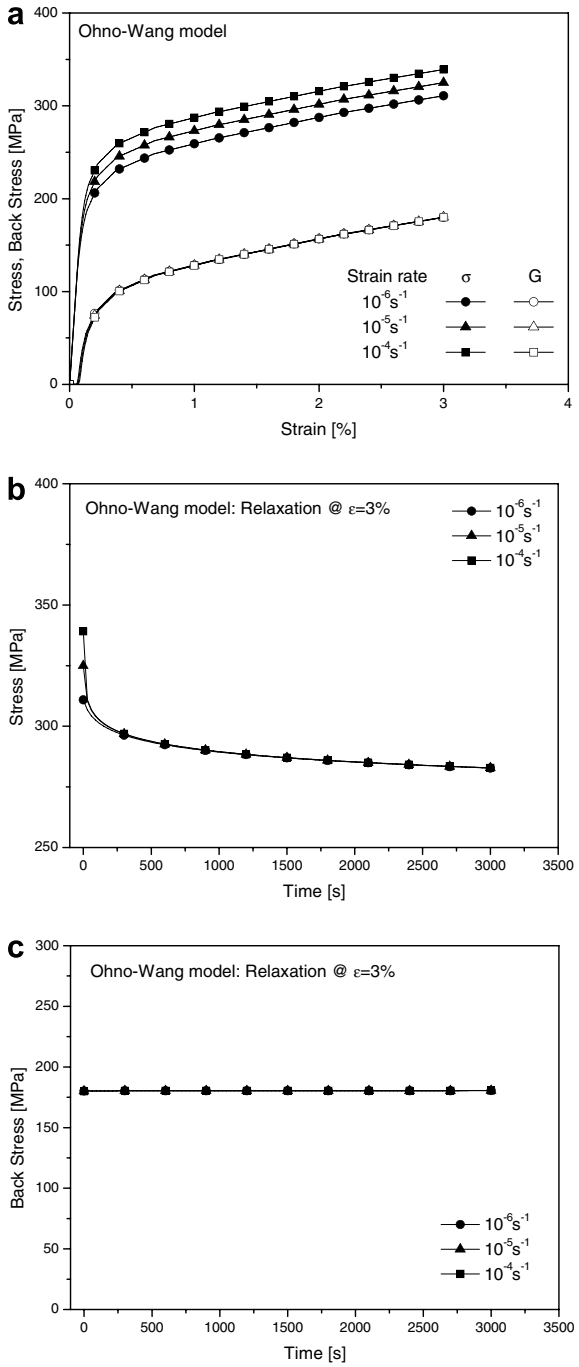

Fig. 3. Numerical experiments by Ohno–Wang model. The back stress is rate-independent during both loading and relaxation. The relaxed stresses end up at one endpoint as shown in (b).

$$\{G - H\} = A \tag{20}$$

Due to the rate independence of H and A, the asymptotic solution of the back stress, applied approximately when the flow stress is reached, appears to be rate-independent.

Under relaxation condition, the back stress rate can be expressed as follows:

$$\dot{G} = -\left[\frac{\psi}{E}\left(\frac{(G-H)}{A}+\frac{E_t}{E}\right)-\frac{E_t}{E}\right]|\dot{\sigma}| \tag{21}$$

When relaxation starts in the region of fully developed inelastic flow, the relations $E_t/E \ll 1$ and $(G-H)/A \approx 1$ are available. We then have $\dot{G} \approx -[(\psi - E_t)/E]|\dot{\sigma}|$. This relation shows that the back stress decreases significantly with time during relaxation period whereas its change was considered to be negligible in the rate-independent NLK model previously discussed. Using the condition $\dot{\varepsilon} = 0$, the magnitude of the stress rate during relaxation becomes $\dot{\sigma} = -EB[(\sigma - G)/K]^m$. Since the overstress $\sigma - G$ increases with strain rate before the beginning of relaxation, the stress and back stress decrease faster with an increase of prior strain rate. Finally, the relaxation terminates when the condition $\sigma - G = 0$ is satisfied.

The material constants used for simulation are:

$$E = 200\ \text{GPa}, \quad E_t = 1000\ \text{MPa}, \quad \psi = 100\ \text{GPa}, \quad A = 250\ \text{MPa}$$
$$B = 3 \times 10^{-3} s^{-1}, \quad K = 100\ \text{MPa}, \quad m = 15$$

In the region of the fully developed inelastic flow, the stress and back stress grow at the same rate that is determined by means of the evolution of the kinematic stress as shown in Fig. 4a. The back stress is independent of the strain rate under loading condition. However, the change of the back stress is apparent during relaxation and the back stress associated with the fastest prior strain rate has the smallest magnitude, see Fig. 4c. In contrast to the previous models, the relaxed stresses shown in Fig. 4b have different end points due to the negative rate sensitivity of the back stress during relaxation period. The stress concerned with a faster prior strain rate has a smaller magnitude at the end of the relaxation periods.

2.3. Rate-dependent NLK model

For the purpose of modeling negative rate sensitivity of the flow stress accompanied by dynamic strain aging, a new nonlinear kinematic hardening rule for the back stress has been proposed by means of introducing a rate sensitivity parameter into the dynamic recovery term of the evolution law for the back stress. The rate sensitivity parameter causing the back stress to be rate-dependent is a repository for modeling negative, zero and positive rate sensitivity in a consistent manner.

To reproduce unusual rate sensitivities concerned with dynamic strain aging, a constitutive model within the framework of VBO was originally proposed in a three-dimensional, total formulation and the evolution laws for the tensor-valued internal state variables of the model were consequently defined as explicit functions of the overstress (Ho and Krempl, 2000, 2001, 2002); however, the stress rate term in the evolution rule for the back stress seemed to be responsible for the conflict with the second law of thermodynamics (Freed et al., 1991; Chaboche, 1993; Krempl, 1996; Hall, 2005). Due to the drawback, the stress rate term was excluded from the evolution rule for the back stress (Ho, 2001) and then constitutive equations were altered into the usual inelastic incompressible, deviatoric formulation in which a concept of yield surface was employed to describe pure, linear elastic region (Ho, 2004, 2006).

In a deviatoric formulation without a yield surface, the evolution of the back stress and the kinematic stress are now defined, respectively, as follows:

$$\dot{\mathbf{g}} = \psi\left[\frac{2}{3}\dot{\mathbf{e}}^{\text{in}} - \frac{(\mathbf{g}-\mathbf{h})}{R}\dot{\phi}\right] + \dot{\mathbf{h}} \tag{22}$$

$$\dot{\mathbf{h}} = \frac{2}{3}E_t\dot{\mathbf{e}}^{\text{in}} \tag{23}$$

where ψ and E_t are material constants, and $\dot{\phi} = B[J(\boldsymbol{\sigma} - \mathbf{G})/K]^m$ is the effective inelastic strain rate. The scalar variable R with the dimension of stress is given by

$$R = r_c + \sqrt{\frac{3}{2}\text{tr}(\mathbf{rr})}; \quad \mathbf{r} = [A + \beta J(\boldsymbol{\sigma} - \mathbf{G})]\frac{(\mathbf{s}-\mathbf{g})}{J(\boldsymbol{\sigma} - \mathbf{G})} \tag{24}$$

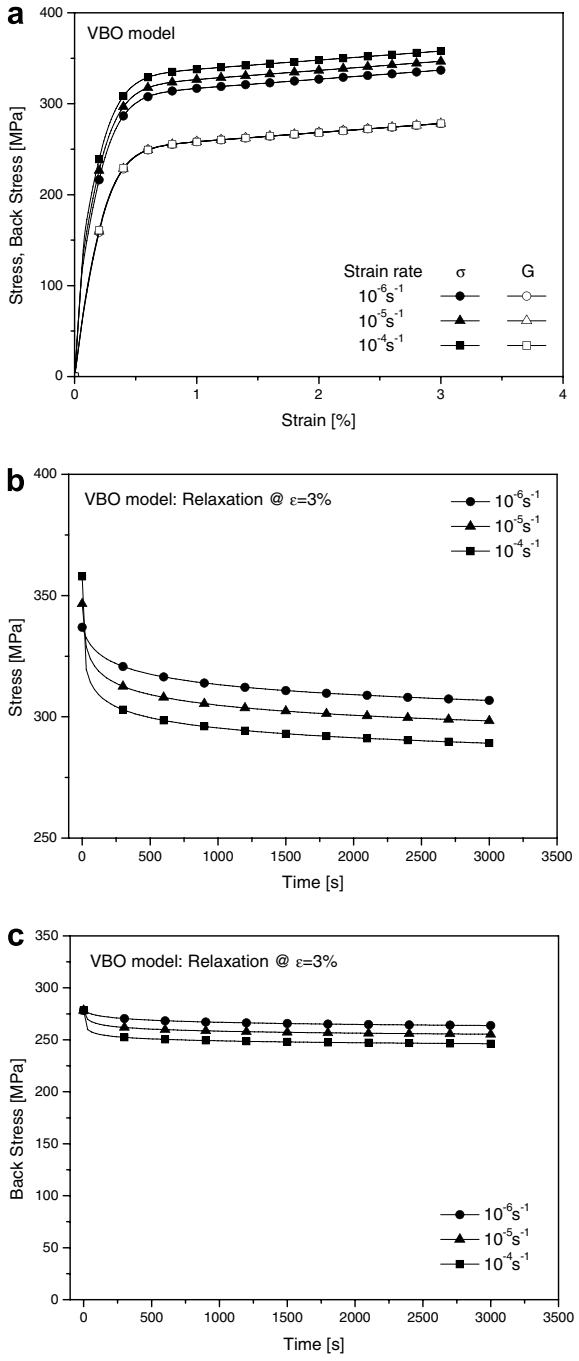

Fig. 4. Numerical experiments by VBO model. (a) Rate-independent back stress during loading; (b) smaller relaxed stress for faster prior strain rate; (c) negative rate sensitivity of back stress during relaxation.

where r_c and A are material constants. Many metallic materials and alloys exhibit the Portevin-LeChatelier effect (PLC) that is attributed to dynamic strain aging. The phenomenon associated with negative strain rate sensitivity of the flow stress generally depends on strain and strain rate in a certain range of temperature. To model these properties, the rate sensitivity parameter β may be defined as a function of the effective inelastic

strain rate and/or the accumulated inelastic strain, see Ho (2001). In this study, the rate sensitivity parameter is kept constant for the sake of convenience.

In case of uniaxial tensile loading, the following asymptotic limits between the internal state variables for $A + \beta\{|\sigma - G|\} > 0$ are valid:

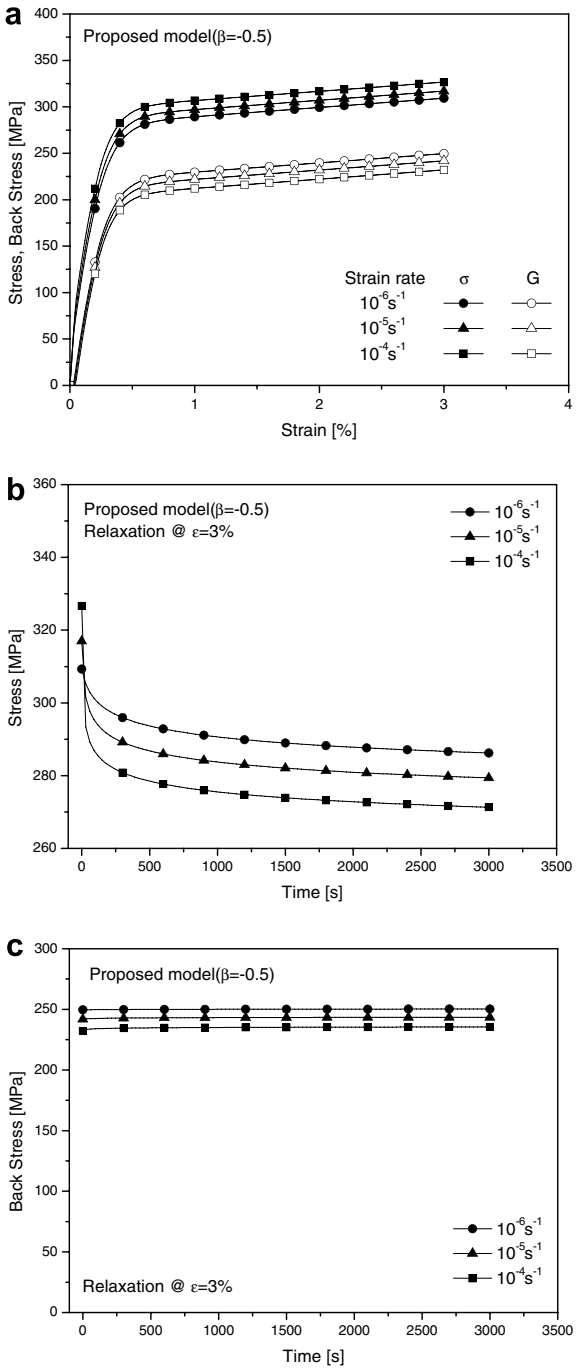

Fig. 5. Numerical experiments by proposed model ($\beta = -0.5$). (a) Rate-dependent (negative) back stress during loading; (b) smaller relaxed stress for faster prior strain rate; (c) negative rate sensitivity of back stress during relaxation.

$$\{G - H\} = r_c + A + \beta\{|\sigma - G|\} \tag{25}$$

$$\{\sigma - H\} = r_c + A + (1 + \beta)\{|\sigma - G|\} \tag{26}$$

To arrive at these relations, $J(\boldsymbol{\sigma} - \mathbf{G}) = |\sigma - G|$ and $\{R\} = r_c + A + \beta\{|\sigma - G|\}$ are utilized. It follows from Eq. (25) that the back stress in the asymptotic state is the sum of the rate-independent contribution

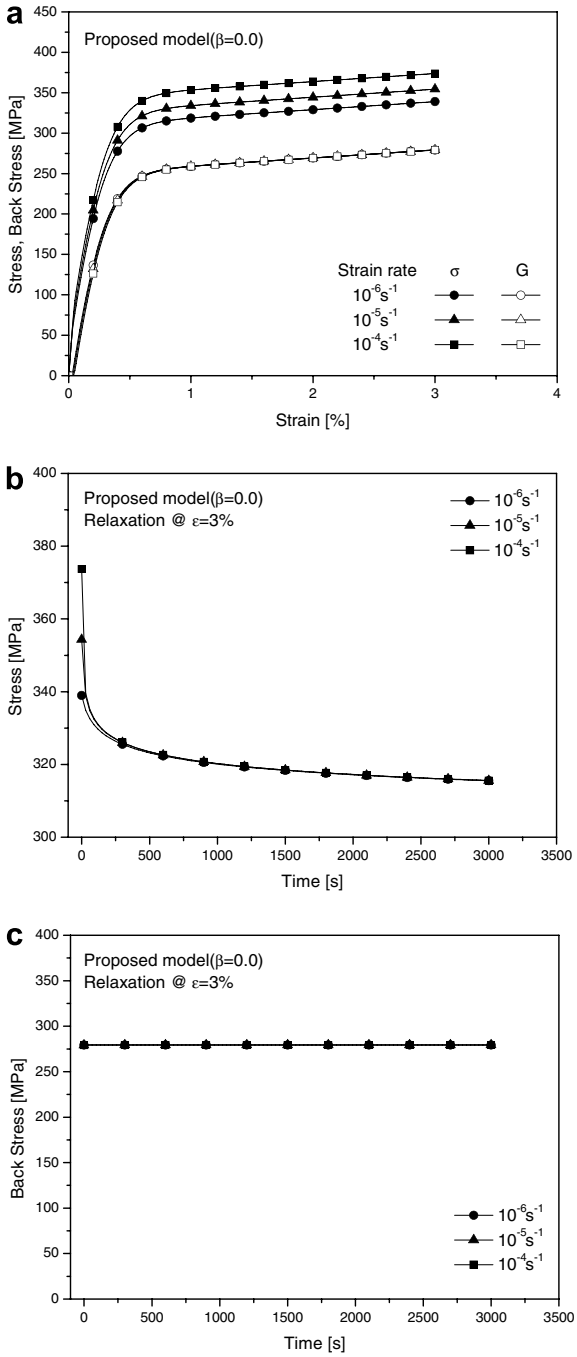

Fig. 6. Numerical experiments by proposed model ($\beta = 0.0$). (a) Rate-independent back stress during loading; (b) no influence of prior strain rate on relaxed stress; (c) rate-independent back stress during relaxation.

$\{H\} + r_c + A$ and the rate-dependent one $\beta\{|\sigma - G|\}$ in which the overstress invariant $\{|\sigma - G|\}$ nonlinearly increases with loading rate.

Depending on the value of β, the back stress can show positive rate sensitivity (back stress increases with an increase of loading rate) for $\beta > 0$, zero rate sensitivity (back stress is independent of loading rate) for $\beta = 0$ like the previously discussed models and negative rate sensitivity (back stress decreases with an increases of

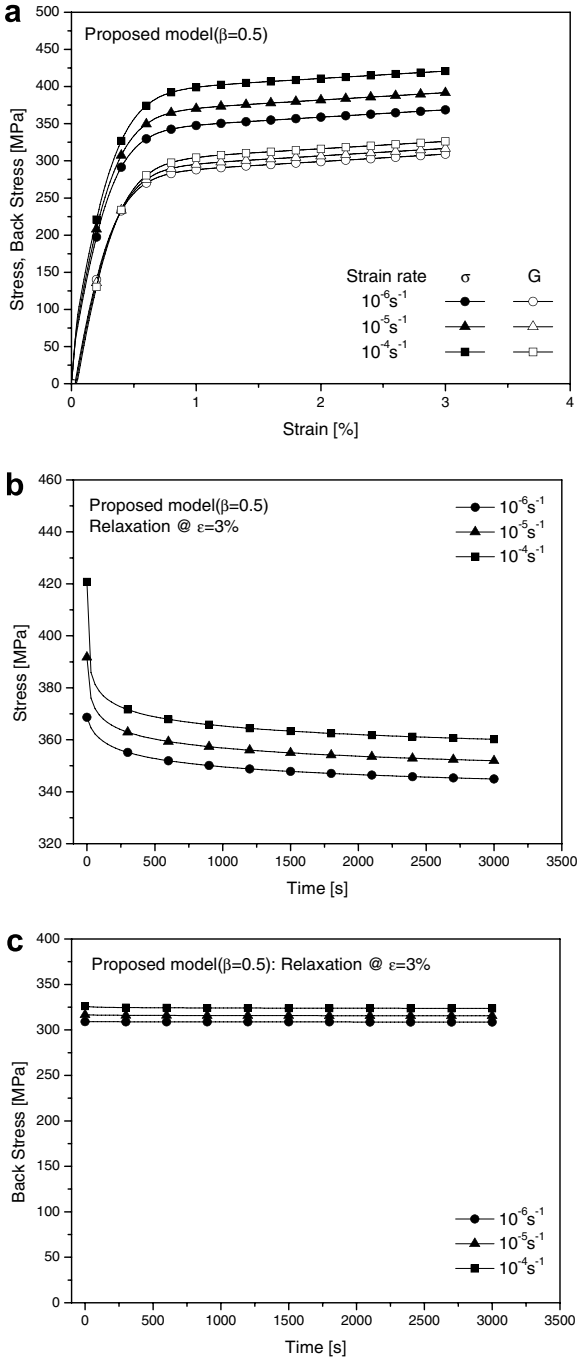

Fig. 7. Numerical experiments by proposed model ($\beta = 0.5$). (a) Rate-dependent (positive) back stress during loading; (b) larger relaxed stress for faster prior strain rate; (c) positive rate sensitivity of back stress during relaxation.

loading rate) for $\beta < 0$. For example, when a value of the rate sensitivity parameter β less than zero is used the rate-dependent contribution term $\beta\{|\sigma - G|\}$ has a minus sign and thus reduces the magnitude of the back stress more for faster strain rate. In the same manner, positive, zero and negative rate sensitivity of the flow stress can be modeled under the condition $\beta > -1$, $\beta = -1$ and $\beta < -1$, respectively, as seen in Eq. (26).

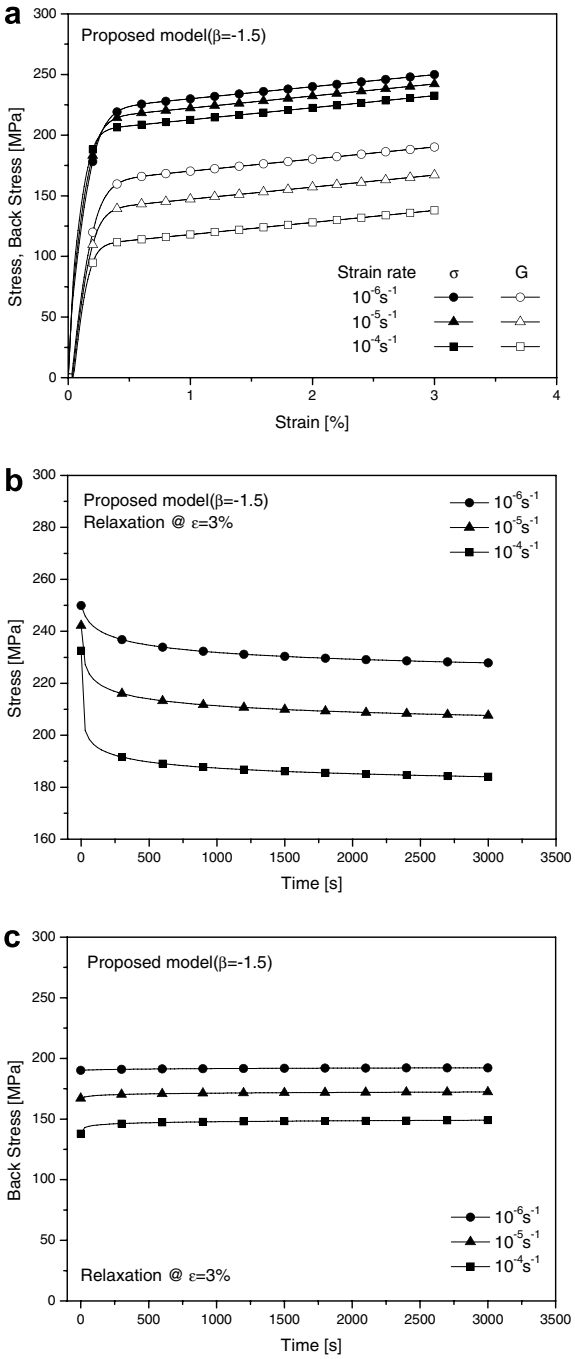

Fig. 8. Numerical experiments by proposed model ($\beta = -1.5$); negative rate sensitivity of flow stress. (a) Rate-dependent (negative) back stress during loading; (b) smaller relaxed stress for faster prior strain rate; (c) negative rate sensitivity of back stress during relaxation.

The changes of the stress and back stress during relaxation period are obtained respectively:

$$\dot{G} = \left[\frac{\psi}{E}\left(1 - \frac{(G-H)}{R}\right) + \frac{E_t}{E}\right]|\dot{\sigma}| \tag{27}$$

$$\dot{\sigma} = -EB\left[\frac{(\sigma - G)}{K}\right]^m \tag{28}$$

It is shown from Eq. (27) that the change of the back stress is very small enough to be neglected since the two conditions $(G-H)/R \approx 1$ and $E_t/E \ll 1$ can be used in the region of fully developed inelastic flow where relaxation takes place. Therefore, a type of rate sensitivity of the back stress experienced during loading is always kept for relaxation period. Eq. (28) shows that the stress drop stops when the stress arrives at the back stress. As a consequence, the relaxed stress at the end of relaxation period depends on prior strain rate. For $\beta < 0$ the relaxed stress associated with the fastest prior strain rate has the smallest magnitude. When $\beta > 0$, on the other hand, the magnitude of the relaxed stress at termination increases with an increase in prior strain rate.

The following material constants are used for the results in Figs. 5–8:

$$E = 200\ \text{GPa}, \quad E_t = 1000\ \text{MPa}, \quad \psi = 190\ \text{GPa}, \quad A = 250\ \text{MPa}$$

$$B = 1 \times 10^{-2} s^{-1}, \quad K = 150\ \text{MPa}, \quad m = 10, \quad r_c = 1\ \text{MPa}$$

For $\beta = -0.5$, Fig. 5a shows the stress and back stress curves for uniaxial tensile loading up to $\varepsilon = 0.03$ with different strain rates. The variations in the stress and the back stress during the subsequent relaxation period are shown in Fig. 5b and c, respectively. It is seen from Fig. 5a that the stress exhibits positive rate sensitivity,

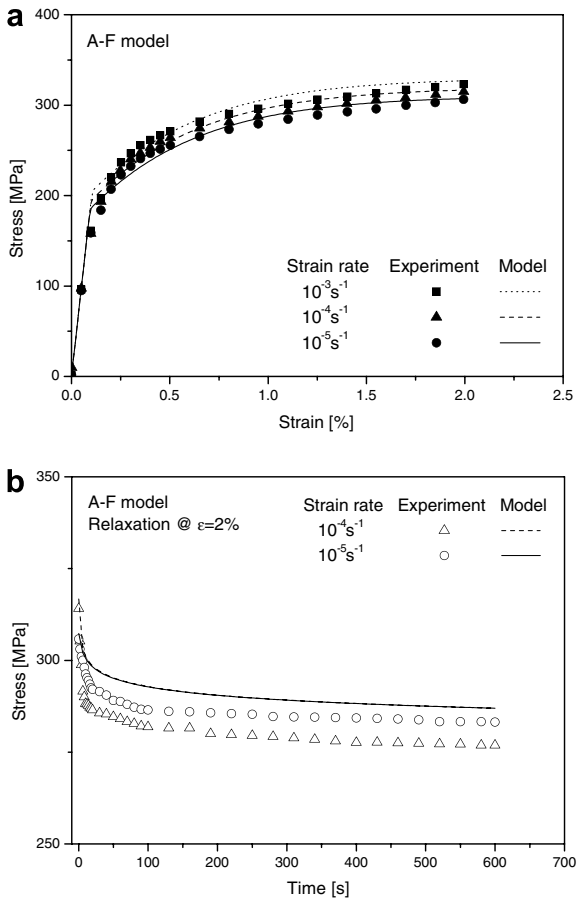

Fig. 9. Simulations by Armstrong–Frederick model.

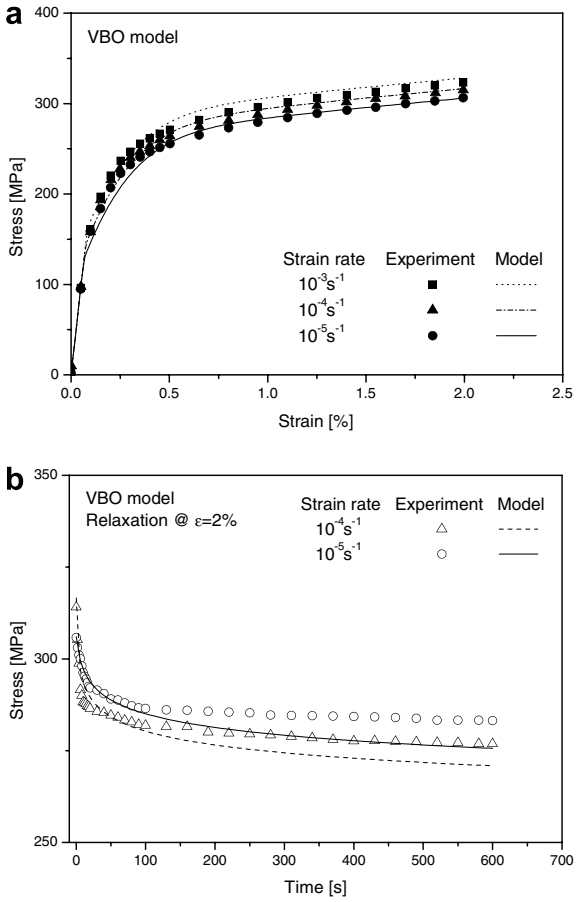

Fig. 10. Simulations by VBO model.

while the back stress shows negative rate sensitivity as expected from Eqs. (25) and (26). However, the back stress in the period of relaxation does not change and maintains the rate sensitivity under the loading condition, see Fig. 5c. Consequently, the relaxed stress associated with the fastest prior strain rate has the smallest magnitude at the end of the relaxation period as shown in Fig. 5b. By setting $\beta = 0$, the model depicts the rate insensitivity of the back stress during both loading and relaxation condition as shown in Fig. 6a and c, respectively. The relaxed stress at the end of relaxation periods has the same property as the rate-independent NLK model, namely, there is no influence of prior strain rate on the relaxed stress level, see Fig. 6b. It is seen in Fig. 7a using $\beta = 0.5$ that both the stress and the back stress exhibit positive rate sensitivity, which is accordance with the prediction of Eqs. (25) and (26). Expected from Eq. (28), the relaxed stress associated with the slowest prior strain rate has the smallest magnitude as seen in Fig. 7b due to the positive rate sensitivity of the back stress during relaxation.

On the other hand, when $\beta = -1.5$ is used both the stress and the back stress exhibit negative rate sensitivity in the fully developed inelastic flow region, see Fig. 8a. It is seen in Figs. 8b and c that the rate-dependent relaxation behavior has the same properties as the case of $\beta = -0.5$ since the back stress has negative rate sensitivity accomplished under the condition of $\beta < 0$.

The modeling capability of the three groups of nonlinear kinematic hardening rules for relaxation behavior is verified by comparing the predictions with experiments of Type 304 stainless steel showing positive rate sensitivity of flow stress. Experimental tests at room temperature were conducted on a MTS810 closed-loop servo-hydraulic testing system with dog-bone type specimens (Ho, 2007). Figs. 9–11 show simulations of the Armstrong–Frederick model ($E = 196$, $K = 151$, $A = 92$, $m = 24$, $C = 25$, $\gamma = 200$), the VBO model ($E_t = 2100$, $\psi = 65$, $A = 180$, $B = 1 \times 10^{-3}$, $K = 110$, $m = 20$) and the proposed model ($E_t = 2100$, $\psi = 100$,

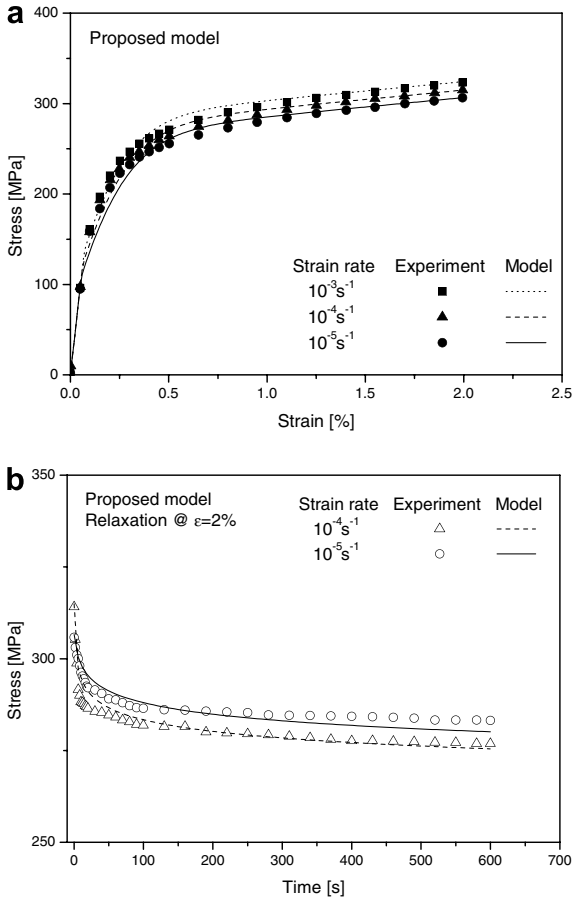

Fig. 11. Simulations by proposed model with $\beta = -0.38$.

$\beta = -0.38$, $A = 198$, $B = 1 \times 10^{-3}$, $K = 140$, $m = 20$, $r_c = 1$), respectively. The Armstrong–Frederick model has no effect of prior strain rate on the relaxed stress at the end of relaxation period. By contrast, the VBO and proposed models predict that the relaxed stress related to the faster prior strain rate has the smaller magnitude. The proposed model is also applied to IN738 at 450 °C reported by Yaguchi et al. (2002); $E = 185$, $E_t = 5000$, $\psi = 700$, $\beta = -1.3$, $A = 785$, $B = 2 \times 10^{-4}$, $K = 200$, $m = 16$, $r_c = 1$. It is shown in Fig. 12a that the model simulates negative rate sensitivity of the flow stress in the fully developed inelastic flow region. The relaxation behavior influenced by prior strain rate is depicted in Fig. 12b.

3. Conclusions

This study categorizes unified constitutive models into three groups from the viewpoint of the rate dependence of the back (equilibrium) stress that is defined by the kinematic hardening rule of the constitutive model. The three groups of the constitutive models are evaluated in terms of numerical experiments for stress relaxation responses to different prior strain rates. Although all groups predict that the magnitude of stress drop increases with an increase of prior strain rate for equal relaxation periods, the influence of prior strain rate on the relaxed stress at the end of relaxation period depends strongly on the rate dependency of the back stress used.

The back stress in the rate-independent NLK model is always independent of strain rate under both loading and relaxation condition. Due to the rate independence of the back stress during relaxation period, it is not possible to predict different end points of the relaxed stresses for equal relaxation periods.

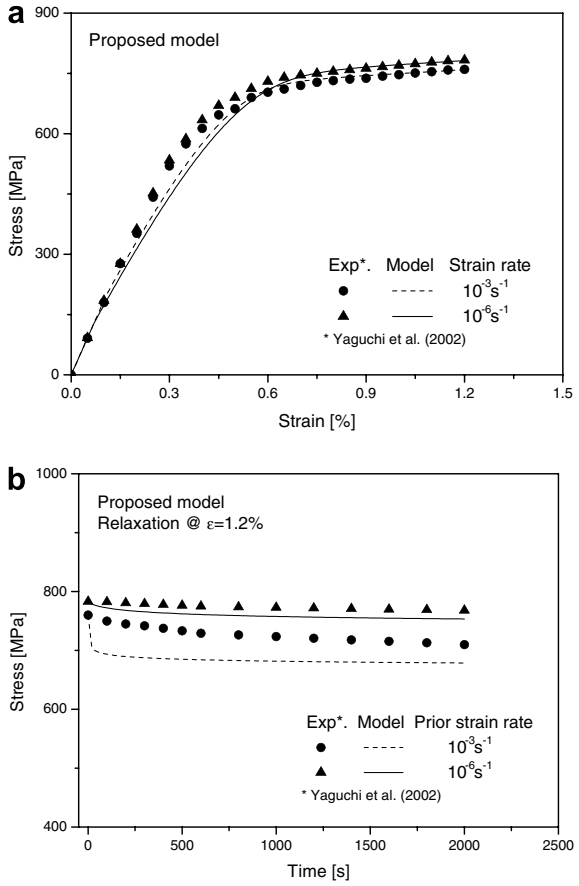

Fig. 12. Simulations by proposed model with $\beta = -1.3$.

In the rate-independent NLK model with a stress rate term, the back stress shows negative rate sensitivity to prior strain rate during relaxation while it is independent of strain rate during loading. The negative rate sensitivity of the back stress causes the relaxed stress associated with the fastest prior strain rate to have the smallest magnitude at the end of relaxation period.

The proposed model introduces a new kinematic hardening rule that makes the back stress be rate-dependent during loading and keep its trend in the rate dependence during relaxation period. The positive, zero and negative rate sensitivity of the back stress, which is determined by the value of the rate sensitivity parameter β, cause the relaxed stress at the end of relaxation period to have larger, constant and smaller magnitude respectively, with an increase of prior strain rate.

To model that the relaxed stress related to the fastest prior strain rate has the smallest magnitude at the end of relaxation period, the back stress under relaxation condition should have negative rate sensitivity to prior strain rate. This requirement is satisfied in the rate-independent NLK model with a stress rate term and the proposed rate-dependent NLK model using the condition of $\beta < 0$.

References

Armstrong, P.J., Frederick, C.O., 1966. A mathematical representation of the multiaxial bauschinger effect (CEGB Report RD/B/N/731). Berkeley Nuclear Laboratories, R&D Department, CA.

Bordonaro, C.M., Krempl, E., 1992. Effect of strain rate on the deformation and relaxation behavior of 6/6 Nylon at room temperature. Poly. Eng. Sci. 32, 1066–1072.

Basuroychowdhury, I., Voyiadjis, G., 1998. A multiaxial cyclic plasticity model for non-proportional loading cases. Int. J. Plast. 14, 855–870.

Chaboche, J.L., Rousselier, G., 1983. On the plastic and viscoplastic constitutive equations, parts I and II. J. Pressure Vessel Tech. 105, 153–164.
Chaboche, J.L., 1986. Time-independent constitutive theories for cyclic plasticity. Int. J. Plast. 2, 149–188.
Chaboche, J.L., Nouailhas, D., 1989. A unified constitutive model for cyclic viscoplasticity and its applications to various stainless steel. J. Eng. Mat. Tech. 111, 424–430.
Chaboche, J.L., 1993. Cyclic viscoplastic constitutive equations, part I: thermodynamically consistent formulations. J. Appl. Mech. 60, 813–821.
Colak, O.U., Krempl, E., 2003. Modeling of uniaxial and biaxial ratcheting behavior of 1026 Carbon steel using the simplified viscoplasticity theory based on overstress (VBO). Acta Mech. 160, 27–44.
Freed, A.D., Chhaboche, J.L., Walker, K.P., 1991. A viscoplasticity theory with thermodynamic considerations. Acta Mech. 90, 155–174.
Hall, R.B., 2005. A thermodynamic framework for viscoplasticity based on overstress (VBO). J. Eng. Mat. Tech. 127, 369–373.
Ho, K., Krempl, E., 2000. Modeling of positive, negative and zero rate sensitivity by using the viscoplasticity theory based on overstyress (VBO). Mech. Time-dependent Mat. 4, 21–42.
Ho, K., 2001. Modeling of nonlinear rate sensitivity by using an overstress model. Comp. Model. Eng. Sci. 2, 351–364.
Ho, K., Krempl, E., 2001. The modeling of unusual rate sensitivities inside and outside the dynamic strain aging regime. J. Eng. Mat. Tech. 123, 28–35.
Ho, K., Krempl, E., 2002. Extension of the viscoplasticity theory based on overstress (VBO) to capture non-standard rate dependence in solids. Int. J. Plast. 18, 851–872.
Ho, K., 2004. A study on strain rate sensitivity by unified viscoplasticity. Trans. Mat. Proc. 13, 600–607.
Ho, K., 2006. Unified constitutive equations of viscoplastic deformation: development and capabilities. JSME Int. J. (Series A) 49, 138–146.
Ho, K., 2007. The rate dependent deformation behavior of AISI type 304 stainless steel at room temperature. Trans. Mat. Proc. 16, 101–106.
Khan, A., Farrokh, B., 2006. Thermo-mechanical response of nylon 101 under uniaxial and multi-axial loadings, part I: experimental results over wide ranges of temperatures and strain rates. Int. J. Plast. 22, 1506–1529.
Krempl, E., Kallianpur, V., 1984. Some critical uniaxial experiments for viscoplasticity at room temperature. J. Mech. Phys. Solids 32, 301–314.
Krempl, E., McMahon, J.J., Yao, D., 1986. Viscoplasticity based on overstress with a differential growth law for the equilibrium stress. Mech. Materials 5, 35–48.
Krempl, E., 1996. A small strain viscoplasticity theory based on overstress. In: Krausz, A., Krausz, K. (Eds.), Unified Constitutive Laws of Plastic Deformation. Academic Press, San Diego, pp. 281–318.
Krempl, E., Nakamura, T., 1998. The influence of the equilibrium stress growth law formulation on the modeling of recently observed relaxation behaviors. JSME Int. J. (Series A) 41, 103–111.
Krempl, E., 2001. Relaxation behavior and modeling. Int. J. Plast. 17, 1419–1436.
Lemaitre, J., Chaboche, J.L., 1994. Mechanics of solid materials. Oxford University Press, Cambridge.
Majors, P., Krempl, E., 1994. The isotropic viscoplasticity theory based on overstress applied to the modeling of modified 9wt.%Cr–1wt.%Mo steel at 538 °C. Mat. Sci. Eng. A186, 23–34.
Ohno, N., Wang, J.-D., 1993. Kinematic hardening rules with critical state of dynamic recovery, part I: formulations and basic features for ratcheting behavior. Int. J. Plast. 9, 375–390.
Ohno, N., Abdel-Karim, M., 2000. Uniaxial ratcheting of 316FR steel at room temperature, part II: constitutive modeling and simulation. J. Eng. Mat. Tech. 122, 35–41.
Phillips, A., Tang, J., Ricciuti, M., 1974. Some new observations on yield surfaces. Acta Mech. 20, 23–39.
Prager, W., 1956. A new method of analyzing stresses and strains in work hardening plastic solids. J. Appl. Mech. 23, 493–496.
Ramaswamy, V., Stouffer, D., Laflen, J., 1990. A unified constitutive model for the inelastic uniaxial response of Rene'80 at temperatures between 538 °C and 982 °C. J. Eng. Mat. Tech. 112, 280–286.
Yaguchi, M., Takahashi, Y., 1999. Unified constitutive model for modified 9Cr–1Mo steel incorporating dynamic strain aging effect. JSME Int. J. (Series A) 42, 1–10.
Yaguchi, M., Takahashi, Y., 2000. A viscoplastic constitutive model incorporating dynamic strain aging effect during cyclic deformation conditions. Int. J. Plast. 16, 241–262.
Yaguchi, M., Yamamoto, M., Ogata, T., 2002. A viscoplastic constitutive model for nickel-base superalloy, part 2: modeling under anisothermal conditions. Int. J. Plast. 18, 1111–1131.